UNIVERSITY OF CALIFORNIA,
IRVINE

Compound Refractive Lenses based on Microspheres for X-ray Beam Manipulation

THESIS

submitted in partial satisfaction of the requirements
for the degree of

BACHELOR OF SCIENCE

in Applied Physics

by

Lisset Sarai Ayala

2020

TABLE OF CONTENTS

	Page
ABSTRACT OF THE THESIS	
INTRODUCTION	1
CHAPTER 1: Conventional X-Ray Sources	3
CHAPTER 2: Laser Compton Source	6
CHAPTER 3: Compound Refractive Lenses	8
CHAPTER 4: Methods	12
CHAPTER 5: Results and Discussion	13
CHAPTER 6: Conclusion	19
BIBLIOGRAPHY	20

ABSTRACT OF THE THESIS

Compound Refractive Lenses based on Microspheres for X-ray Beam Manipulation

by

Lisset Sarai Ayala

Bachelor of Science in Applied Physics

University of California, Irvine, 2020

Professor Christopher Barty

X-ray sources are an advantageous tool in clinical medicine for diagnosing and treating disease. However, a consequence of obtaining an x-ray image is exposing the patient to harmful radiation. Synchrotron-like radiation, produced by compact laser Compton light sources, has been shown to enhance the resolution of x-ray images while reducing the amount of radiation exposed to the patient using quasi-monochromatic x-rays [1-5]. Laser Compton sources emit a beam whose divergence depends upon the energy used in their production. It is possible to focus and collimate x-ray beams using refractive optics [6]. Low Z materials are usually considered for x-ray refractive lenses due to their relatively low absorption. Refraction of X-rays has been demonstrated using spherical hole lenses in low Z blocks [6], but inconsistencies during the drilling process can alter how the beam is focused. In this thesis, a compound refractive lens composed of a high density, low Z liquid material with polystyrene microsphere inclusions is proposed. Simulation studies are presented that show the feasibility of using spherical, liquid refractive lenses to manipulate x-rays.

INTRODUCTION

X-ray imaging has played a critical role in diagnostic medicine and surgery since the early 20th century. One of the advantages of X-ray imaging is that a reliable image can be taken quickly, aiding in the process to identify abnormalities, diagnosing potential diseases, and leading image guided procedures. The effects of treatment and contrast dye can also be captured in real time as they are being injected, a technique often used in fluoroscopy to examine bodily functions [1] and Digital Subtraction Angiography to examine vascular structures [2]. While conventional x-ray imaging is well established and readily available in clinical settings it also offers a number of drawbacks concerning image quality and patient safety. These drawbacks, such as unnecessary radiation exposure due to beam hardening [3], can be addressed using a synchrotron to generate a quasi- monochromatic x-ray beam.

Synchrotron radiation has been shown to produce finer and more detailed x-ray images while simultaneously exposing the patient to less radiation compared to conventional x-ray sources [2-4]. However, the cost and size of synchrotron facilities make them impractical for clinical use. Laser Compton sources can produce synchrotron-radiation-quality x-rays at a fraction of the size of a synchrotron facility and have also been shown to be beneficial in producing more detailed images while also delivering smaller radiation doses to patients [1-4]. A focused beam could further increase the resolution of images and aid in radiotherapy.

The method of using a compound refractive lenses (CRL) to focus an x-ray beam was first introduced in 1998 [5]. Since then, refractive lenses have been a useful tool for focusing hard x-rays to a spot size in the micrometer range. One of the simplest methods for manufacturing this lens involves drilling a series of holes into a block of low Z material, such as Aluminum and Beryllium. Alternatively, lenses can be produced using microfabrication via deep x-ray lithography onto sheets of polymethylmethacrylate (PMMA) [7]. The array of holes forms a series of concave "lenses," making a compound refractive lens. If fabricated improperly, a costly consequence of this method can be the deformation of the material.

Another suggested method for fabricating a CRL consists of plastic microspheres immersed in a low Z liquid within a thin capillary tube [5]. The plastic spheres will shape the low Z material into a series of uniform biconcave "lenses." Also, drilled hole lenses only focus in one dimension, requiring two lenses placed perpendicularly to focus the beam in x and y-planes. With spherical lenses each lens focuses in both planes, focusing the beam in two-dimensions with less lenses [8]. While other compound refractive lenses have been successful in focusing x-rays, a compound refractive lens based on microspheres serves as a lower-cost method that improves the CRL geometry while providing the same focusing benefits.

In this thesis, various low-Z refractive lens materials are evaluated for 33keV x-ray focusing. A simulation of a compound refractive microsphere lens was developed using the ray tracing code, Optica, in order to observe the focal lengths and beam transmission through different materials. The results are comparable to formulae estimates given by the compound refractive lens simulator, XOP2.4.

CHAPTER 1 CURRENT X-RAY SOURSES

There are several modalities in radiology that use conventional x-ray tubes to produce x-rays such as fluoroscopy, mammography, and computed tomography. The x-ray generating components of an x-ray tube consist of a generator, a cathode, and an anode within a vacuum enclosure, as seen in Figure 1. X-rays are produced when the energy released from excited electrons is converted into electromagnetic radiation [9]. This is done by heating and exciting the cathode to release a cloud of free electrons through thermionic emission; the number of electrons emitted is limited by the amount of current the cathode can handle [9]. The anode attracts and decelerates the electrons as they approach the Tungsten nuclei, converting the loss of kinetic energy into electromagnetic radiation in the form of bremsstrahlung and characteristic radiation [10]. The area where the emitted electron beam impacts the anode is referred to as the focal spot of the electron

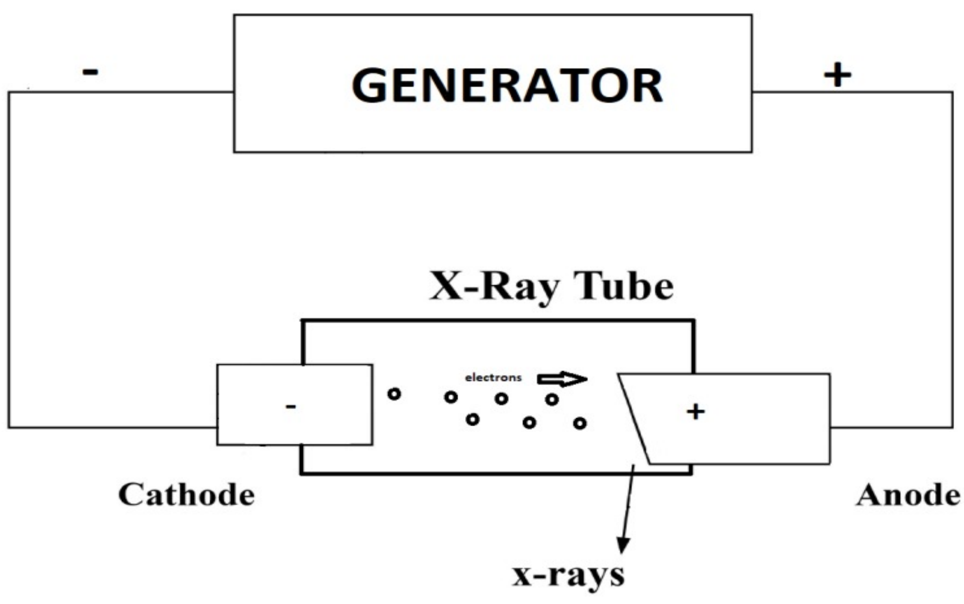

Figure 1: X-ray generator and tube. Dawood Tafti, C.V.M. Radiation X-ray Production 2019

beam and it determines the intensity of the x-ray beam [8]. Bremsstrahlung radiation constitutes the majority of x-rays produced from an x-ray tube, resulting in a polychromatic spectrum of x-ray energy [9]. In the vacuum enclosure, electrons are approaching and interacting with the anode at different distances and depths, generating photons with varying amounts of energy. In particular, electrons that come extremely close to the nuclei experience a greater decelerating effect, due to the greater electrostatic attraction between the electron and nucleus, create higher energy photons [10]. As the emitted photons pass through an object, ones with a lower energy are attenuated more than higher energy photons. This change in the x-ray spectrum as it travels through a medium is referred to as beam hardening [10].

Photons of various energies will interact with the anatomical structure of the patient differently; they will either be absorbed, scattered, or transmitted through the patient. Beam hardening can interfere with both the image quality and radiation dose level affecting the patient. X-ray interactions in matter include coherent scattering, Compton scattering, and photoelectric absorption [8]. Coherent scattering occurs when a low energy photon collides with and rebounds off an orbital electron, only changing direction and not ionizing the atom; this results in only a small dose of radiation to the patient [9]. Compton scattering occurs when a high energy photon collides with and removes an orbital electron from its shell, ionizing the atom and scattering the photon. This is disadvantageous because scattered photons leaving the material will darken and fog the x-ray image, affecting the quality of the image and will require exposing the patient to more radiation [10]. In photoelectric absorption, an incident photon collides with an inner-shell electron and is completely absorbed, ejecting the electron and ionizing the atom. The scattered electron will not escape the patient, and while this improves image quality by limiting the number of photons to fog the image, it increases the amount of radiation absorbed by the patient [10]. The intensity of the x-ray beam can be manipulated by adjusting the size of the focal spot on the anode target in the x-ray tube.

The source size of the X-ray beam on the anode is similar to the electron spot size at the interaction point on the cathode filament where thermionic emission occurs. Within a focusing cup, cathodes consist of a small and large coiled Tungsten filament. The size of the focal spot is directly related to the size of the filament [9]. A large filament and focal spot create wide, poorly aligned electron beams that generate wide, poorly aligned x-ray beams at the anode. This is beneficial for imaging larger sections of the body that require longer exposures but results in a lower spatial resolution that affects the quality of the image [8]. Smaller filaments and source sizes create narrow, tightly aligned electron beams that at the anode generate narrow, tightly aligned x-ray beams. While this improves the spatial resolution of the image, it is limited by the amount of current the anode can withstand, decreasing the intensity the x-ray beam could potentially provide [9]. Thus, smaller filaments are only used on smaller sections that can be examined with shorter exposures.

The process of producing x-ray photons in an x-ray tube is inefficient. A majority of the kinetic energy from the accelerating electrons is converted into heat, leaving only a small portion to be converted into x-rays [10]. Additionally, conventional x-ray sources produce a polychromatic spectrum of x-rays, creating lower energy photons that are not beneficial for imaging and expose the patient to excess radiation. Beam hardening and the limited size of the focal spot also affect image quality. These issues can be addressed using a Laser Compton source that generates a quasi- monochromatic beam of x-rays by

Compton scattering. A monochromatic x-ray beam of sufficient energy will not expose the patient to harmful low energy radiation which is otherwise absorbed and does contribute to image formation. A laser Compton source has already been shown to be beneficial in several imaging applications [1-4].

CHAPTER 2 LASER COMPTON SOURCE

Synchrotron radiation, produced at a synchrotron source, is highly brilliant [11]. Electrons are accelerated around an electron storage ring at nearly the speed of light, steered by a series of magnets. As the electron changes direction within the magnetic field, it emits bremsstrahlung radiation. At high enough speeds this results in x-rays that can be described as a quasi- monochromatic or coherent beam [12]. Use of synchrotron radiation in medical imaging has shown great potential for improving soft-tissue contrast in x-ray imaging [1-3]. Two methods proposed are K-edge subtraction and phase-contrast imaging.

Digital subtraction imaging is an important image-guided procedure used in the treatment and diagnosis of cardiovascular disease. A contrast agent, usually containing Iodine, is used to increase the contrast between vascular structures and bone surrounding the heart. A series of images are taken before and after the contrast is injected. This process lasts a few seconds and occurs repeatedly during the procedure, exposing the patient to multiple doses of radiation in one session. Motion artifacts such as patient movement and breathing can limit the image resolution, especially when imaging smaller capillaries. K-edge subtraction (KES) imaging follows the same concept of subtraction angiography. KES utilizes the distinct absorption coefficient of a contrast agent to obtain images just below and above the K-edge energy of that contrast agent [2]. Instead of taking images before and after the contrast has been injected, two images at different x-ray energies are taken simultaneously after the injection. The attenuation coefficients of the surfaces not containing the contrast agent are nearly identical between the two energies. When the two images are subtracted these features will completely remove and only the contrast agent image will remain [12]. Acquiring the images simultaneously reduces radiation dose from exposure time and eliminates potential motion artifacts that would otherwise interfere with image production. A comparison between KES with conventional imaging used in neurovascular imaging demonstrated that imaging with monochromatic x-rays reduced patient exposure risk while achieving higher quality images [13]. This is significant for imaging smaller vessels that may be overlooked using conventional imaging due to patient movement and image quality. Another study done at the European Synchrotron Radiation Facility (ESRF), which reviewed coronary imaging around the K-edge of Iodine, arrived at the same conclusion [14].

Fluoroscopy is also an important image-guided procedure that examines dynamic bodily processes. Multiple images that are taken in real time as the process is occurring, essentially producing a video and exposing the patient to multiple doses of radiation in one procedure. Phase- contrast imaging takes advantage of the unique refraction properties of different material to provide contrast between them. The strong difference in phase properties between tissues results in excellent phase contrast. This can be beneficial for examining soft tissues composed of fat, muscle, and other organs which are often laid over each other. In mammography studies, this has beneficial in detecting tumors and abnormal cysts that were embedded within the breast tissue [15, 16].

Currently, research in these fields is limited due to the lack of access to a monochromatic beam source. Laser Compton sources, which can produce synchrotron-like monochromatic x-ray beams, could provide a more compact and affordable solution.

At a Laser Compton source, x-rays are generated by Compton scattering of laser light with an electron beam that has been accelerated by several 10's of MeV energy [17]. In a synchrotron source, GeV-scale electrons oscillate within the changing magnetic field of an undulator with cm-scale magnet spacing. In a laser Compton source, electrons oscillate under micro-scale electro-magnetic field of the laser. Laser photons are scattered by the relativistic electron beam and gain momentum in the direction of the electron beam [18].

The relativistic electrons produce photons in a forward cone beam. This beam is not only quasi-monochromatic but also exhibits partial spatial coherence due to its small source size [17]. A focused beam could further increase the spatial resolution of images and aid in radiotherapy such as Auger cascade therapy and pencil beam stereotactic radio-therapy. Compound refractive lenses consisting of a linear array of concave low-Z material lenses have been shown to focus hard x-rays in one or two dimensions at synchrotron x-ray facilities [8]. With some adjustments it could be feasible to use similar refractive lenses for laser Compton x-ray sources.

CHAPTER 3 COMPOUND REFRACTIVE LENS

In refractive optics, x-rays are guided by refraction at surfaces between different materials. This effect can be described with Snell's law. The index of refraction for x-rays can be written as

$$n = 1 - \ \delta + i\beta$$

where

$$\delta = \frac{N_a \lambda^2 \rho Z r_o}{2\pi A}$$

$$\beta = \frac{\lambda\mu}{4\pi}$$

Here, N_a is Avogadro's' number, λ is the photon wavelength, ρ is the density of the material, r_o is the classical electron radius, Z is the atomic weight, A is the atomic number, and μ is the absorption coefficient of the material. The refractive index decrement δ describes the strength of the refraction and the absorption index β pertains to the x-ray absorption of the material [19]. For compound material the index of refraction can be described as

$$\delta = \frac{N_a \lambda^2 \rho r_o}{2\pi} \frac{\sum_i n_i Z_i}{\sum_j n_j A_j}$$

The real part of the index of refraction for x-rays is less than one. Looking at Snell's Law,

$$n_1 \sin(\theta_1) = n_2 \sin(\theta_2)$$

if the x-ray beam is coming from a vacuum it will refract away from the surface normal, unlike visible light [20]. Thus, multiple concave lenses with a small radius of curvature must be stacked in order to achieve a refracting effect instead of a convex lens.

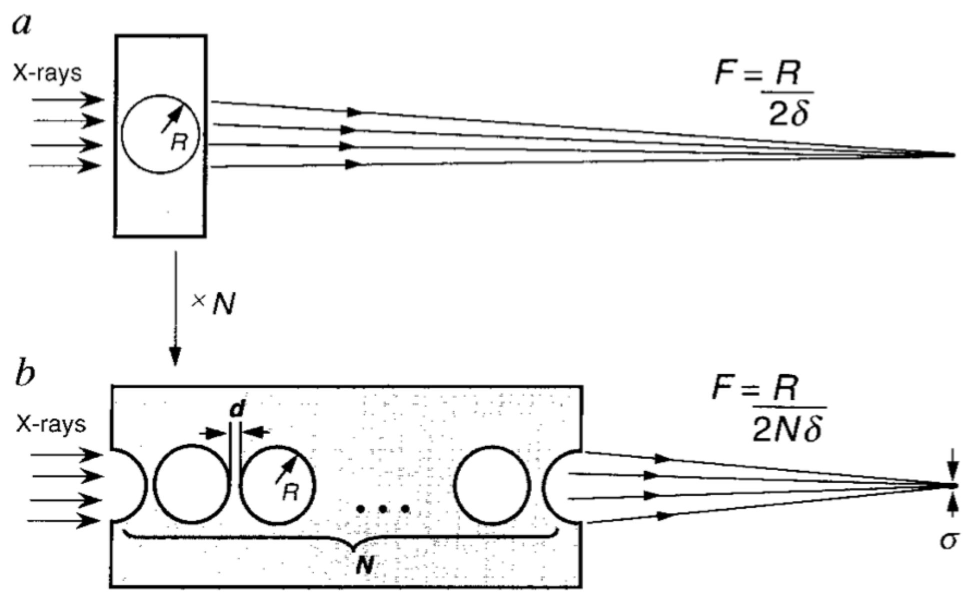

Figure 2: Schematic showing the concept of x-ray focusing by a compound refractive lens. X-ray lenses fabricated by deep x-ray lithography.

Ignoring spherical aberration, a compound lens with N holes will have a focal length of

$$f = \frac{R}{2\delta N}$$

Where R is the radius of the hole, often within the range of micrometers to millimeters, and d is the spacing between the holes [21].

Spherical aberration can be neglected in the case of compound lenses with parabolic holes. Spherical lenses will show strong spherical aberration if the transmission is high, in this case the focal length depends on the position where the incident rays hit the surface of the first lens, and can be described as

$$f = \frac{\sqrt{R^2 - y^2}}{2\delta N}$$

[21]. Transmission of a linear array of spherical lenses is characterized by the absorption in the lens,

$$T \cong e^{-\mu N d}$$

where d is the distance between the holes of the lens [22].

CHAPTER 4 METHODS

A compound refractive lens based on microspheres was designed and simulated using Optica, an optical design software based in Mathematica. Each sphere was created with two cylindrical concave lenses with radii of 750μm and apertures of 1.5mm. The lens pairs were placed 40μm apart to replicate a microsphere lens thickness of 20μm. These parameters were considered based on Du's paper detailing the production of microspheres used in inertial confinement fusion (ICF) target fabrication [23]. The incoming x-ray beam was assumed to be monoenergetic and its energy was set to 33keV, which is the k-edge energy of Iodine, a contrast agent commonly used in fluoroscopy and K-edge subtraction [2]. These parameters were also considered for the XOP2.4 simulations.

Calculations comparing the refractive properties of different material were used to determine what materials could be used for the microsphere shell and liquid surrounding. Simulation were done with shells composed of each liquid agent listed in Table 1. Calculations included solving for the refractive index and expected focal length of each material. Linear absorption coefficients were determined via interpolation of experimentally determined absorption vs. photon energy data points at 33keV provided by the National Institute of Standards and Technology (NIST) Physical Measurement

Laboratory. These values were used to determine the focal length, CRL length, and beam transmission of a lens made from each material.

The results were used to decide which agents are suitable for constructing a microsphere CRL. The results were compared with estimates given by XOP2.4, an x-ray-oriented program with a CRL parameter calculator add-on.

CHAPTER 5: RESULTS AND DISCUSSION

Presented are the calculated and simulated results of a compound refractive lenses considering: (1) the lens parameters needed to achieve a focal length of one meter with lenses of radius 750μm, and (2) a CRL consisting of N=50 holes, each having a radius of 750μm, which were spaced 10μm apart. In a microsphere CRL, the distance between the holes would be width of two microsphere shells adjacent to each other. For simulation purposes, the distance was set to 10μm with the approximation that the absorption from the microsphere shell is negligible to the overall absorption of the lens. Various low-Z materials were tested for their lens length, focal length, and transmission. The liquid materials chosen were water, benzene, carbon tetrachloride, barium sulfate, liquid iodine, diethyl ether, methanol, and ethanol. They are compared to beryllium, carbon, boron, and aluminum, which are materials that have been used to create block compound refractive lenses. Table 1 shows their respective decrements and linear absorption coefficients. The calculated results were used to set the lens parameters for the Optica simulation, which was written in conjunction with the researching post-doctorate.

We can estimate the number of holes needed to fabricate a CRL that could focus a beam to one meter and its lens length using

$$N = \frac{R}{2f\delta}$$

$$l = N(2R + d)$$

Where d is the distance between the lenses.

Material	*Interpolated Linear Attenuation Coefficient (1/cm)*	*XOP2.4 Linear Attenuation Coefficient (1/cm)*	*Calculated decrement*	*XOP2.4 Decrement*	*Density (g/cm3)*
Beryllium	0.3177	0.3205	3.12E-07	3.13E-07	1.848
Diamond	0.5403	0.5333	4.30E-07	4.30E-07	1.70
Boron	0.4606	0.4573	4.13E-07	4.13E-07	2.37
Aluminum	2.371	2.396	4.95E-07	4.97E-07	2.699
Water	0.3387	0.3289	2.11E-07	2.12E-07	0.9971
Benzene	0.219	0.2146	1.80E-07	1.97E-07	0.8765
Carbon Tetrachloride	2.712	2.768	2.93E-07	2.93E-07	1.594
Barium Sulfate	20.89	21.71	7.62E-07	7.51E-07	4.5
Iodine	25.15	26.25	6.29E-07	5.74E-07	3.96
Diethyl Ether	0.1987	0.1828	1.54E-07	1.59E-07	0.7137
Methanol	0.2407	0.2340	1.70E-07	1.69E-07	0.7914
Ethanol	0.2274	0.2231	1.69E-07	1.70E-07	0.7893

Table 1: Calculated decrements and linear absorption coefficients interpolated from database holdings provided by NIST at ~33kEv compared to the values determined by XOP2.4

Considering the lens parameters to achieve a focal length of one meter described in Table 2, it can be observed that the liquid materials require more holes than solid material. As a result, a CRL composed with microspheres can be over twice as a long as a solid block CRL with the same radius. The length of the lens could be decreased by reducing the radius of the holes. While adjusting the radius may be easier to manipulate for drilling holes into a block of material, it poses a greater risk for hole deformation. Microspheres of uniform sphericity and thickness can be produced by manipulating the density during the curing process of production via microencapsulation [24].

Material	Number of lenses	CRL length (m)	Transmission (%)
Beryllium	1202	1.85	68.27
Diamond	872	1.34	62.45
Boron	909	1.40	65.79
Aluminum	758	1.17	16.58
Water	1776	2.74	54.79
Benzene	2087	3.21	63.31
Carbon Tetrachloride	1279	1.97	3.116
Barium Sulfate	492	0.76	3.433E-03
Iodine	596	0.98	3.107E-05
Diethyl Ether	2433	3.75	61.60
Methanol	2210	3.40	58.74
Ethanol	2225	3.43	60.28

Table 2: Calculated lens length and transmission for a focal length of one meter at 33keV

For a CRL of 50 holes with a radius of 750μm the lens length would approximately be 7.5cm. This length more realistic for use in a medical facility but accommodating the focal length may pose an issue. Barium sulfate displays the shortest focal length at the expense of attenuating the x-ray beam more heavily. Whereas benzene transmits most of the beam with a longer focal length. A shorter CRL results in a longer focal length, which elongates the entire beam path. The focal length and lens size are easily adjustable by adding or removing microspheres. The microspheres will be aligned in a plastic capillary tube, where the distance between each hole will be twice the width of the microsphere shell. This shows potential for materials with similar properties to be used as a liquid refractive lens.

Material	Calculated focal length (m)	Simulated Transmission (%)
Beryllium	24.02	98.42
Carbon	17.43	97.33
Boron	18.18	97.72
Aluminum	15.16	88.82
Water	35.52	98.32
Benzene	41.74	98.91
Carbon Tetrachloride	25.58	87.32
Barium Sulfate	9.84	35.19
Liquid Iodine	11.92	28.44
Diethyl Ether	48.66	99.01
Methanol	44.20	98.80
Ethanol	44.51	98.87

Table 3: Focal lengths and transmission for 50 lenses of radii 750μm for different material

The intensity profiles for this CRL using material with lower densities, such as water and ethanol, display the highest transmission but experience a low beam reshaping effect. Barium sulfate and carbon tetrachloride reshape and focus the beam well at the expense of a greater beam attenuation. Figures 5-6 show the corresponding the intensity profiles for the spherical lenses at 33keV.

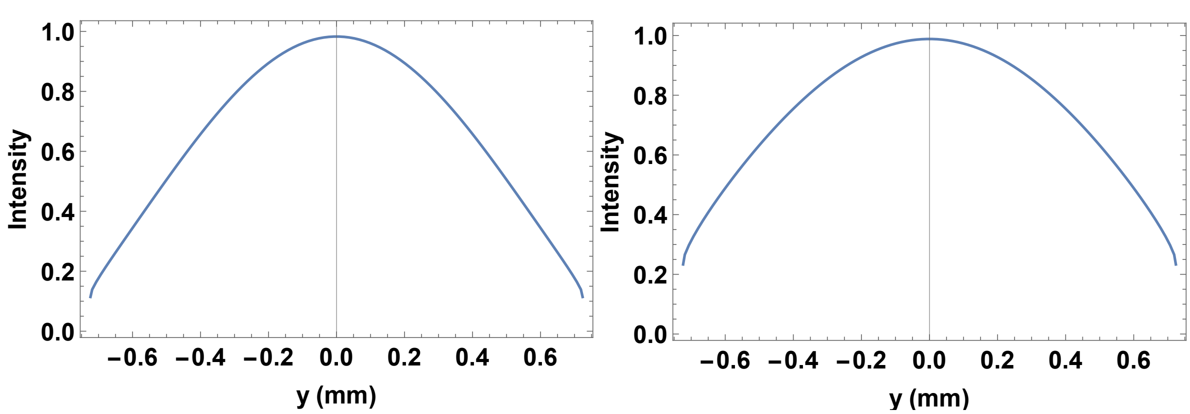

Figure 3: Intensity profiles of water and ethanol respectively. Lighter density materials have a high transmission rate but experience a spherical aberration

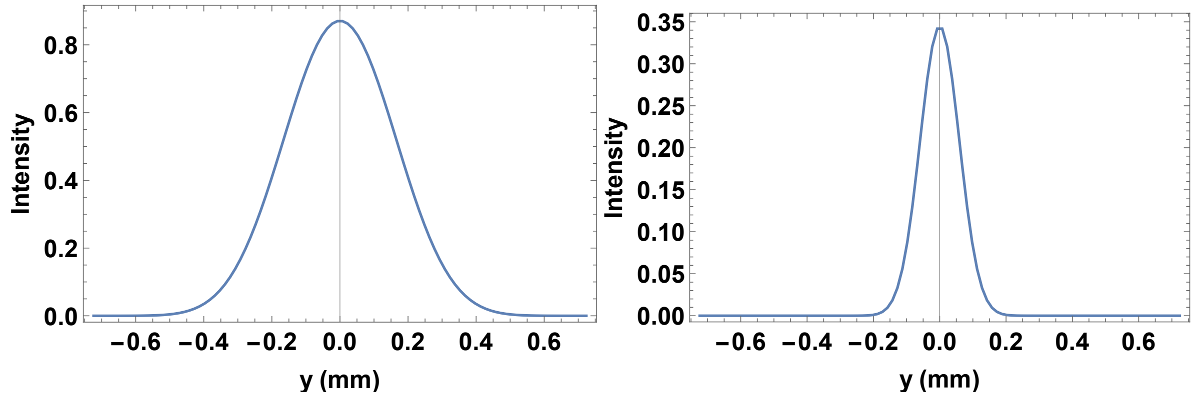

Figure 4: Intensity profiles of carbon tetrachloride and barium sulfate showing their respective beam shaping effects. Increasing the density minimizes the effects of spherical aberration at the expense of a higher beam attenuation

Beam Divergence

In considering the focusing properties of a compound refractive lens, it is important to examine the x-ray beam profile from the laser Compton source. For simulation purposes, the x-ray was assumed to be a parallel, monochromatic beam. However, laser Compton x-rays have a divergence. Figure 6 shows at 30keV only a small percentage of the initial beam is focused by the CRL because of the high divergence of the initial beam. Specifically, about 0.1% of the beam would enter a lens with an aperture of 1.5mm located two meters form the source [25]. Increasing the electron energy can decrease the divergence of the beam, allowing more x-rays to enter the aperture of the CRL. In this case, a larger percentage of the diverging beam would enter the CRL. If the CRL is placed one focal distance from the laser Compton source, the beam would exit the CRL collimated. This collimated beam could be focused using another compound refractive lens, or a collimated beam could also be used as is for pencil beam radiation therapy and other imaging procedures.

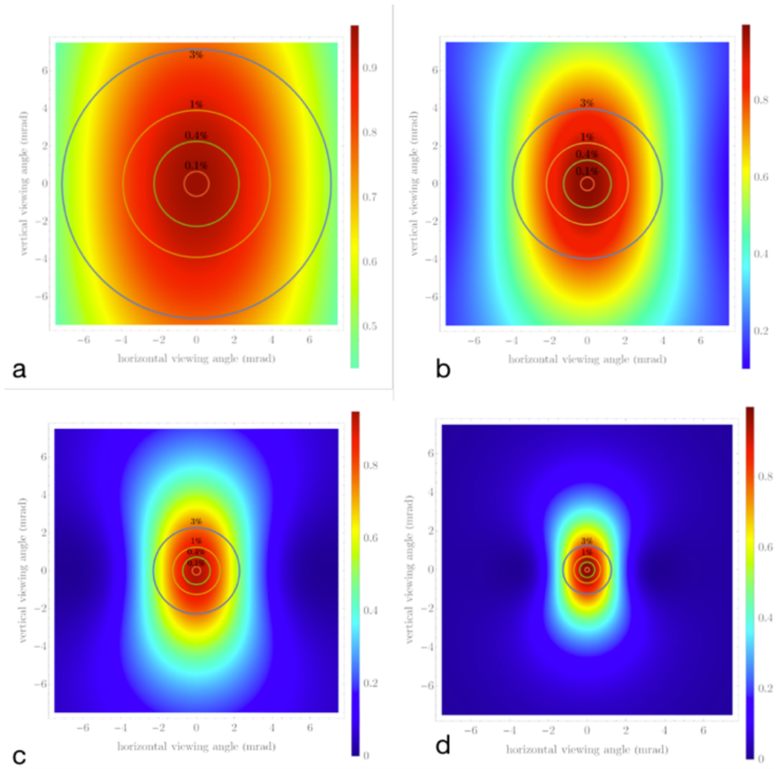

Figure 5: Radiation patterns for photon energies ranging from 30 keV (left), 100 keV, 300 keV, to 1 MeV (right). X-Ray Optics Design Review Report. 2020.

Lens Fabrication

One mechanism used to fabricate microspheres is microencapsulation. This can be done using a triple orifice droplet generator made from syringes or a 3D printed microfluidic device. Microencapsulation involves coating liquid droplets, usually water, in a polymeric film. During the curing process the liquid solution inside the film evaporates while the polymeric film hardens, forming the microsphere shell. Looking at Figure 7, synthesis occurs in the droplet generator. There are multiple factors that influence the deformation of the droplets. Matching the density among the phases of production can improve uniform sphericity and wall thickness of a batch of shells. [26]. Varying the rotation rate during the curing process can also improve the uniform sphericity of the batch [24]. Polystyrene microspheres can be produced in compact spaces and be readily accessible with this process.

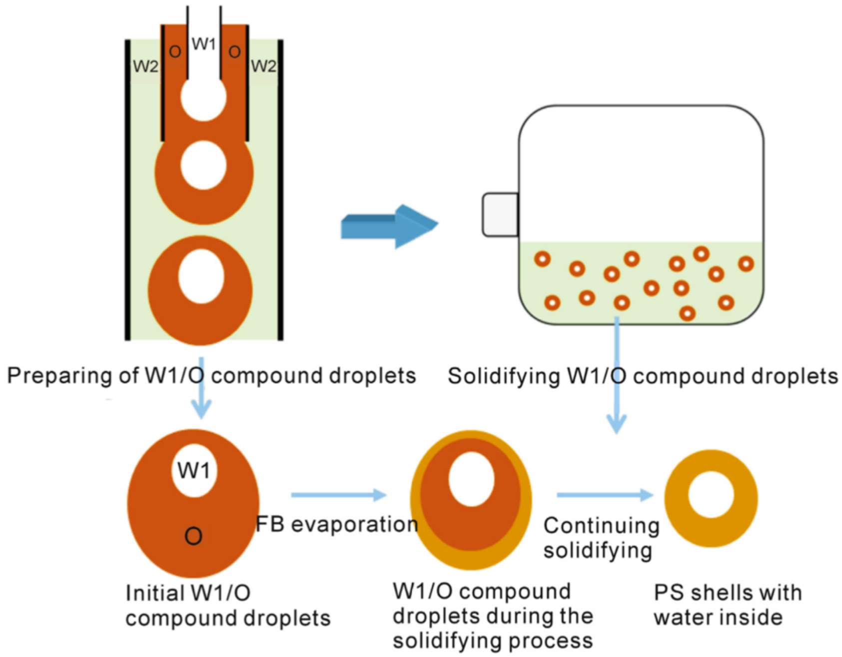

Figure 6: Production of microspheres via microencapsulation. A liquid solution, W1, is encapsulated in a polymetric solution O. The W1/O compound droplet is cured in an alcohol solution W2, where W1 is evaporated leaving an O shell. Investigation of spherical and concentric mechanism of compound droplets

It is also important to consider the viability of the liquid material for a compound refractive lens. It may not be suitable to use material with a low boiling point, is carcinogenic, or does not react well with air or plastic. The simulations show potential for liquid refractive lenses with similar properties to the ones already tested in this study. Further studies can be done with other liquids to test for their refractive properties and viability to be used in a medical facility.

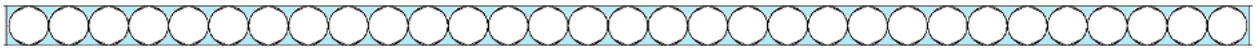

Figure 7: Sideview of a compound refractive lens diagram with polystyrene spheres (outlined in black) within a liquid refractive material (shaded in blue)

CONCLUSION

A detailed analysis of the lens array performance shows that it is possible to fabricate liquid refractive lenses using microspheres for manipulating high-energy x rays. A CRL can focus a collimated beam and has potential to collimate a diverging beam from a laser Compton source. The fabrication of the microspheres is straightforward and inexpensive, and the alignment would be simple with a capillary tube. The focal length and size are easily adjustable by adding or removing microspheres. At 33keV, the manipulated x-ray beam can be used with an Iodine-containing contrast agent to aid in image-guided procedures and radiation therapy.

BIBLIOGRAPHY

1. Gradl, R., et al., *In vivo Dynamic Phase-Contrast X-ray Imaging using a Compact Light Source.* Sci Rep, 2018. **8**(1): p. 6788.
2. Kulpe, S., et al., *K-edge subtraction imaging for coronary angiography with a compact synchrotron X-ray source.* PLoS One, 2018. **13**(12): p. e0208446.
3. Eggl, E., et al., *Mono-Energy Coronary Angiography with a Compact Synchrotron Source.* Sci Rep, 2017. **7**: p. 42211.
4. Labriet, H., et al., *Significant dose reduction using synchrotron radiation computed tomography: first clinical case and application to high resolution CT exams.* Sci Rep, 2018. **8**(1): p. 12491.
5. Haijo Jung, H.-J.K., Eun-Kyung Kim, Jin-O Hong, Jung Ho Je, Yeukuang Hwu, Wen-Li Tsai, Giorgio Magaritondo, and Hyung-Sik Yoo, *Comparison of Unmonochromatized Synchrotron Radiation and Conventional X-rays in the Imaging of Mammographic Phantom and Human Breast Specimens: A Preliminary Result.* Yonsei Medical Journal, 2005. **46**.
6. Snigirev, A., et al., *A compound refractive lens for focusing high-energy X-rays.* Nature, 1996. **384**(6604): p. 49-51.
7. Derrick C. Mancini, N.M., Ralu Divan, Francesco DeCarlo, Judith Yaeger, *X-ray lenses fabricated by deep x-ray lithography.*
8. A. Snigirev, V.K., I. Snigireva, A. Souvorov, B. Lengeler, *Focusing high-energy x rays by compound refractive lenses.* Applied Optics, 1998.
9. Dawood Tafti, C.V.M. *Radiation X-ray Production* 2019.
10. Serman, N., *Production of X-rays and Interactions of X-rays with Matter.* p. 11-20.
11. Munro, I.h., and G.v. Marr., *Synchrotron Radiation Sources*, in *Handbook on Synchrotron Radiation*. 1987.
12. Hwang, Y., *Characterization and Applications of Laser-Compton X-ray Source*, in *Department of Physics* 2018, University of California, Irvine
13. Schü ltke E, F.S., Kelly M, Griebel R, Juurlink B, LeDuc G, *The potential for neurovascular intravenous angiography using K-edge digital subtraction angiography.* Nuclear Instruments ans Methods in Physics Research, 2005.
14. Elleaume, H., *First human transvenous coronary angiography at the European Synchrotron Radiation Facility.* Physics in Medicine and Biology, 2000.
15. Sharma, R., et al., *Phantom-Based Feasibility Studies on Phase-Contrast Mammography at Indian Synchrotron Facility Indus-2.* J Med Phys, 2019. **44**(1): p. 39-48.
16. E. Castelli, P.M.T., MD F. Arfelli, PhD, *Mammography with Synchrotron Radiation: First Clinical Experience with Phase-Detection Technique.* Radiology, 2011. **259**.
17. Kuroda, R., et al., *Quasi-monochromatic hard X-ray source via laser Compton scattering and its application.* Nuclear Instruments and Methods in Physics Research Section A: Accelerators, Spectrometers, Detectors and Associated Equipment, 2011. **637**(1): p. S183-S186.
18. Gibson, D.J., *A High-Energy, Ultrashort-Pulse X-Ray System for the Dynamic Study of Heavy, Dense Materials.* University of California Davis, 2004.
19. Bruno Lengeler, C.S., Johannes TuÈmmler, Boris Benner, Matthias Richwin, Anatoly Snigirev, Irina Snigirevab, Michael Drakopoulosb, *Imaging by Parabolic Refractive Lenses in the Hard X-Ray Range.* Journal of Synchrotron Radiation, 1999.
20. Johannes, T.D.-P., *Development of CRL for Hard X-Rays.* 2000.
21. Lengeler, B., et al., *Transmission and gain of singly and doubly focusing refractive x-ray lenses.* Journal of Applied Physics, 1998. **84**(11): p. 5855-5861.

22. M.A. Piestrup, H.R.B., C.K. Gary, J.T. Cremer, R.H. Pantell, R. Tatchyn, *Compound refractive lenses for novel X-ray sources.* Nuclear Instruments and Methods in Physics Research, 2001.
23. Du, K., et al., *Recent progress in ICF target fabrication at RCLF.* Matter and Radiation at Extremes, 2018. **3**(3): p. 135-144.
24. Han, X., et al., *Improvement of the Sphericity and the Thickness Uniformity of the Polystyrene (PS) Shell Microsphere during Curing Process.* Coatings, 2019. **9**(6).
25. Ferenc Raksi, F.H., Yoonwoo Hwang, Michael Jentschel, Chris Barty, *X-Ray Optics Design Review Report.* 2020.
26. Liu, M., et al., *Investigation of spherical and concentric mechanism of compound droplets.* Matter and Radiation at Extremes, 2016. **1**(4): p. 213-223.